Journal of Porphyrins and Phthalocyanines
J. Porphyrins Phthalocyanines 2013; **17**: 1120–1128
DOI: 10.1142/S1088424613500788

Published at http://www.worldscinet.com/jpp/

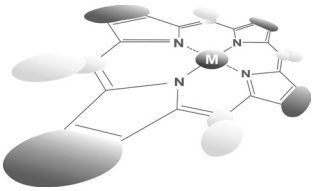

Demetalation kinetics of the zinc chlorophyll derivative possessing two formyl groups: effects of formyl groups conjugated to the chlorin macrocycle on physicochemical properties of photosynthetic pigments

Kana Sadaoka[a], Toru Oba[b], Hitoshi Tamiaki[c], Shigenori Kashimura[a] and Yoshitaka Saga*[a◊]

[a] *Department of Chemistry, Faculty of Science and Engineering, Kinki University, Higashi-Osaka, Osaka 577-8502, Japan*
[b] *Department of Material and Environmental Chemistry, Graduate School of Engineering, Utsunomiya University, Utsunomiya, Tochigi 321-8585, Japan*
[c] *Graduate School of Life Sciences, Ritsumeikan University, Kusatsu, Shiga 525-8577, Japan*

Received 8 May 2013
Accepted 2 June 2013

ABSTRACT: Demetalation kinetics of zinc chlorophyll derivative **1** possessing two formyl groups directly linked to the A- and B-rings of the chlorin macrocycle, which was synthesized from chlorophyll *b*, was examined under acidic conditions and compared with those of Zn chlorins **2** and **3** possessing a single formyl group in the A- and B-ring, respectively, as well as Zn chlorin **4** lacking any formyl group to unravel the substitution effects on demetalation properties of chlorophyllous pigments. Demetalation kinetics of diformylated Zn chlorin **1** was slower than those of monoformylated Zn chlorins **2** and **3**, indicating that the effect of the electron-withdrawing formyl group on demetalation kinetics was amplified by introduction of two formyl groups to the chlorin macrocycle. High correlations were observed between demetalation rate constants of Zn chlorins **1–4** and the sum of Hammett σ parameters of the 3- and 7-substituents on the chlorin macrocycle, indicating that the combination of electron-withdrawing abilities of the substituents linked directly to the cyclic tetrapyrrole was responsible for demetalation properties of zinc chlorophyll derivatives.

KEYWORDS: chlorophyll, formyl group, hammett constant, pheophytinization.

INTRODUCTION

Chlorophyll (Chl) molecules are crucial pigments in photosynthesis. Naturally occurring Chls have structural diversity in terms of the tetrapyrrole macrocycles and their peripheral substituents [1, 2]. Figure 1a depicts molecular structures of Chls, whose macrocycles are chlorin-type (17,18-dihydroporphyrin), in oxygenic photosynthetic organisms. The most abundant Chl pigment is Chl *a*, which functions in both capture of sunlight and charge separation using the light energy. Chl *a* has aliphatic substituents (2-methyl, 3-vinyl, 7-methyl, and 8-ethyl groups) in the A- and B-rings of the chlorin macrocycle.

Chl molecules possessing a formyl group directly linked to the chlorin macrocycle are of great importance in efficient light-harvesting activities in photosynthetic organisms [1–5]. Three kinds of Chls, namely Chls *b*, *d*, and *f*, are present in oxygenic photosynthetic organisms. In Chl *b*, the formyl group is occupied at the 7-position in the B-ring of the chlorin macrocycle. Such 7-formylated chlorin-type pigments are also found as bacteriochlorophyll(BChl)s *e* and *f* in green sulfur photosynthetic bacteria [6–8]. Chls *d* and *f* have the

◊SPP full member in good standing

*Correspondence to: Yoshitaka Saga, email: saga@chem.kindai.ac.jp

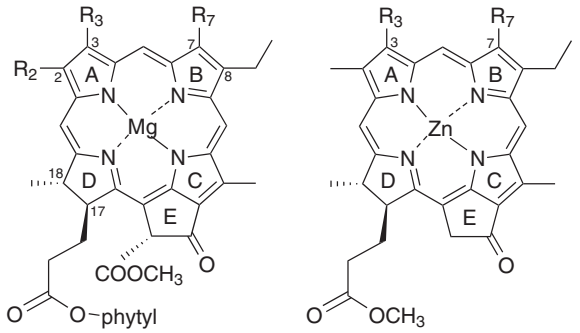

Pigment	R_2	R_3	R_7
Chl *a*	CH_3	$CH{=}CH_2$	CH_3
Chl *b*	CH_3	$CH{=}CH_2$	CHO
Chl *d*	CH_3	CHO	CH_3
Chl *f*	CHO	$CH{=}CH_2$	CH_3

(a)

Compound	R_3	R_7
1	CHO	CHO
2	CHO	CH_3
3	$CH{=}CH_2$	CHO
4	$CH{=}CH_2$	CH_3

(b)

Fig. 1. Molecular structures of natural chlorin-type chlorophylls in oxygenic photosynthetic organisms (a) and synthetic Zn chlorins **1–4** used in this study (b). The corresponding free-bases of the latter were represented as **1′–4′**

formyl group at the 3- and 2-positions, respectively, in the A-ring [3–5]. The formyl groups conjugated to the chlorin macrocycle are responsible for spectral and physicochemical properties. In natural photosynthetic systems, these formylated Chl molecules can harvest light-energy, which is hardly absorbed by Chl *a*, because of the shifts of the absorption bands compared with Chl *a*. Therefore, physicochemical studies on formylated Chls have attracted considerable attentions in the research area of photobiology.

Recently, a Chl molecule possessing two formyl groups called 7-formyl-Chl *d* was successfully biosynthesized in a mutant of *Acaryochloris marina*, in which a Chl *a* oxygenase was expressed [9, 10]. This novel pigment exhibits unique spectral features, in which the Soret absorption band (470 nm in acetone) is shifted to a longer wavelength than those in Chls *b* and *d*, whereas the Q_y-band (672 nm in acetone) is positioned between those of Chls *b* and *d*. The analysis of photosystem(PS)-II complexes isolated from the mutant demonstrated that the diformylated Chl molecules occupied the binding sites of Chl *d* and functioned as light-harvesting pigments [10]. The physicochemical properties and metabolism of such a diformylated Chl have emerged as contribution for elucidation of photosynthetic mechanisms, as well as developments of artificial photoactive nanodevices. However, the content of the diformylated Chl in the mutant of *Acaryochloris marina* is quite low (*ca*. 4% of total biosynthesized Chls) at the stationary phase [9], and its model pigments will be useful in this research area. Here, we synthesize Zn chlorin **1** possessing two formyl groups at the 3- and 7-positions (Fig. 1b) and analyze its physicochemical properties on removal of the central metal from the chlorin macrocycle to afford the corresponding free-base **1′**.

Demetalation of natural Chls called pheophytinization is one of the key reactions in photosynthetic metabolisms. Photosynthetically active (B)Chl molecules lacking the central metal, namely pheophytin (Phe) *a* and bacteriopheophytin (BPhe) *a*/*b*, function as the primary electron acceptor in PS II-type photosynthetic reaction centers [11–17], but biosynthesis of the (B)Phe molecules has not completely been unraveled. Removal of the central metal from chlorophyllous pigments is also of biological importance in the early stage of Chl degradation, but this mechanism is still enigma [11, 18–21]. Additionally, pheophytinization of chlorophyllous pigments has also attracted much attention for researchers engaged in photosynthetic research, since this reaction is one of the major denaturation phenomena in laboratories. Therefore, physicochemical analyses of demetalation of natural Chls and synthetic metallochlorins have extensively been performed [22–39].

Formyl groups directly linked to the chlorin macrocycle remarkably affect kinetic stability to demetalation of chlorophyllous pigments [22–24, 27, 28, 30–32, 34, 35, 39]. Mackinney and Joslyn first reported the difference of demetalation kinetics between Chl *a* possessing the 7-methyl group and Chl *b* possessing the 7-formyl group [22, 23], and this difference was confirmed by other reports [24, 28, 32]. The effect of the 7-formyl group on slow demetalation kinetics was also found in the 13^2-stereoisomer of Chl *b* (Chl *b′*), BChl *e* in green sulfur photosynthetic bacteria, and synthetic Zn methyl pyropheophorbide *b* [27, 28, 30, 31, 34]. The formyl group at the 3-position in the chlorin macrocycle is also reported to contribute to resistance against removal of the central metal [32, 35, 39]. In contrast to these reports on demetalation properties of monoformylated metallochlorins, there is no information on demetalation properties of diformylated chlorophyllous pigments. Comparison of demetalation properties of diformylated Zn chlorin **1** with those of monoformylated Zn chlorins **2** and **3** as well as Zn chlorin **4** possessing no formyl group allows us to understand effects of formyl groups conjugated to the cyclic tetrapyrrole on removal of central metal from the chlorin ring more deeply.

RESULTS AND DISCUSSION

Synthesis and spectral properties of diformylated chlorins

The free-base chlorin **1′** possessing two formyl groups at the 3- and 7-positions was synthesized by oxidation of the 3-vinyl group in methyl pyropheophorbide *b* (**3′**), followed by zinc insertion into its chlorin macrocycle to afford diformylated Zn chlorin **1**. The two compounds **1**

and **1′** were identified by ^{1}H NMR and HRMS (see Experimental section). Visible absorption spectra of Zn chlorin **1** and free-base chlorin **1′** were compared with other Zn chlorins **2–4** and the corresponding free-base chlorins **2′–4′**, respectively, in Fig. 2. Zn chlorin **1** exhibited the Soret and Q_y absorption bands at 463 and 659 nm, respectively, in acetone (Fig. 2a). The Soret band of diformylated **1** was red-shifted compared with monoformylated **2** and **3** by 20 and 12 nm, respectively. The Q_y-band of **1** was shifted to a longer wavelength than that of 7-formylated **3** by 22 nm, but was shifted to a shorter wavelength by 21 nm than that of 3-formylated **2**. The relative ratio of the Q_y absorbance over the Soret absorbance of diformylated **1** was 0.26, which was analogous to that of 7-formylated **3** (the relative ratio was 0.30). Such spectral features of **1** corresponded to those of the novel 7-formyl-Chl *d* biosynthesized in the mutant of *Acaryochloris marina* [9] as summarized in Table 1. These indicate that diformylated Zn chlorin **1** should be a good model pigment of 7-formyl-Chl *d*. Free-base chlorin **1′** showed essentially the same tendencies as Zn chlorin **1** as shown in Fig. 2b.

Table 1. Summary of λ_{max} differences between diformylated and monoformylated pigments at the Soret and Q_y positions

	$\Delta\lambda_{max}$ (Soret), nm	$\Delta\lambda_{max}$ (Q_y), nm	Reference
λ_{max}(**1**) – λ_{max}(**2**)	20	-21	this work
λ_{max}(**1**) – λ_{max}(**3**)	12	22	this work
λ_{max}(7-formyl-Chl *d*) $-\lambda_{max}$(Chl *d*)	23	-21	[9] and [40]
λ_{max}(7-formyl-Chl *d*) $-\lambda_{max}$(Chl *b*)	13	21	[1] and [9]

Spectral changes through demetalation

Demetalation of synthetic Zn 3,7-diformyl-chlorin **1** was kinetically analyzed in acidic aqueous acetone. Figure 3 depicts a spectral change of Zn 3,7-diformyl-chlorin **1** during the demetalation process in aqueous acetone (acetone/water = 3/1, vol/vol) at the proton concentration of 1.8×10^{-1} M. The 472-nm Soret absorption band of Zn 3,7-diformyl-chlorin **1** gradually decreased and a new absorption band of demetalation product, namely **1′**, appeared at 451 nm. The Q_y absorbance of **1** at 666 nm also decreased with an increase of the 676-nm Q_y absorbance of **1′**. The small bands in the wavelength range between 500 and 650 nm of Zn chlorin **1** also gradually changed. This spectral change exhibited the isosbestic points at 461, 508, 563, and 674 nm.

Spectral changes of the other Zn chlorins were essentially the same as that of **1** (data not shown). The Soret bands of demetalation products of **2–4** were shifted to shorter wavelengths than those of the Zn chlorins (**2**: 450 → 430 nm, **3**: 459 → 437 nm, **4**: 430 → 414 nm). These allow us to analyze their demetalation reactions quantitatively by monitoring absorbance changes at the Soret peak positions of Zn chlorins **1–4**.

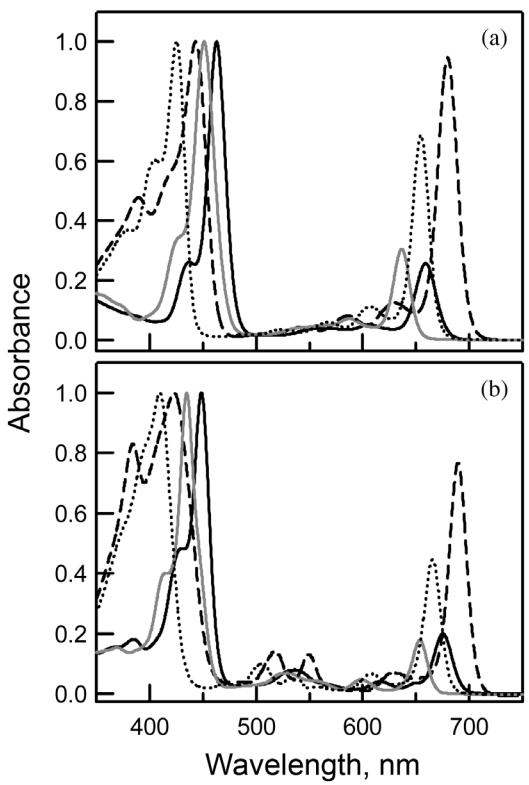

Fig. 2. Visible absorption spectra of Zn chlorins **1–4** (a) and free-base chlorins **1′–4′** (b) in acetone. **1** and **1′**: black solid curve. **2** and **2′**: broken curve. **3** and **3′**: gray solid curve. **4** and **4′**: dotted curve. The spectra were normalized at the Soret peak positions

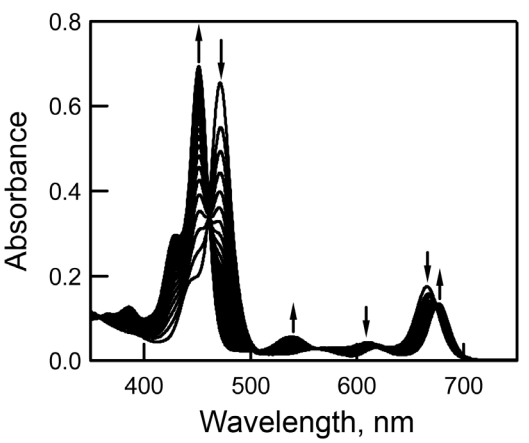

Fig. 3. Spectral changes of Zn 3,7-diformy-chlorin **1** in acetone/water (3/1, vol/vol) at the proton concentration of 1.8×10^{-1} M. Spectra were measured from 0 to 23 h at a 30-min interval. The arrows show the directions of absorbance changes

Demetalation kinetics

Figure 4 depicts time courses of Soret peak absorbances of Zn formylated chlorins **1–3** through demetalation at the proton concentration of 1.8×10^{-1}, 1.2×10^{-1}, and 6.0×10^{-2} M. All the kinetic plots exhibited linear relationships between the logarithm of Soret absorbance and reaction time. Therefore, the demetalation reactions of Zn chlorins **1–3** can be regarded as pseudo-first-order reactions. These are consistent with the reaction conditions, in which the proton concentration was much higher than the concentration of Zn chlorins. Demetalation rate constants, *k*s, were determined by fitting the time courses of Soret absorbance of Zn chlorins **1–3** to the following kinetic equation:

$$\ln [(A-A_\infty)/(A_0-A_\infty)] = -kt, \quad (1)$$

where A_0, A, and A_∞ are Soret absorbance of **1–3** at the onset of the measurement, at time t, and at the complete demetalation, respectively. Demetalation rate constants of Zn formylated chlorins **1–3**, which were the averages of more than three independent measurements, are plotted in Fig. 5 against the proton concentrations. It is worthy noting that the standard deviations were within 5, 4, and 10% of the averaged values of demetalation rate constants for **1**, **2**, and **3**, respectively. Demetalation rate constants of **4** at the proton concentration of 6.0×10^{-2} M were also estimated from the kinetic plots in the same manner as **1–3**, and the averaged value is plotted in Fig. 5, but kinetic analysis cannot be performed at higher proton concentrations because of significantly fast demetalation kinetics of **4**. The logarithm of the demetalation rate constants, log *k*, of Zn chlorins **1–3** increased linearly with log [H^+]. The slopes of log *k* of Zn formylated chlorins **1–3** against log [H^+] in Fig. 5 were estimated to be 2.9, 3.0, and 2.9, respectively. These values were slightly larger than those of Zn chlorin **2** (the slope was 2.6) in a previous report [39]. The difference of the slope in log [H^+]–log *k* plots between the present study and the previous report [39] might be derived from the examined

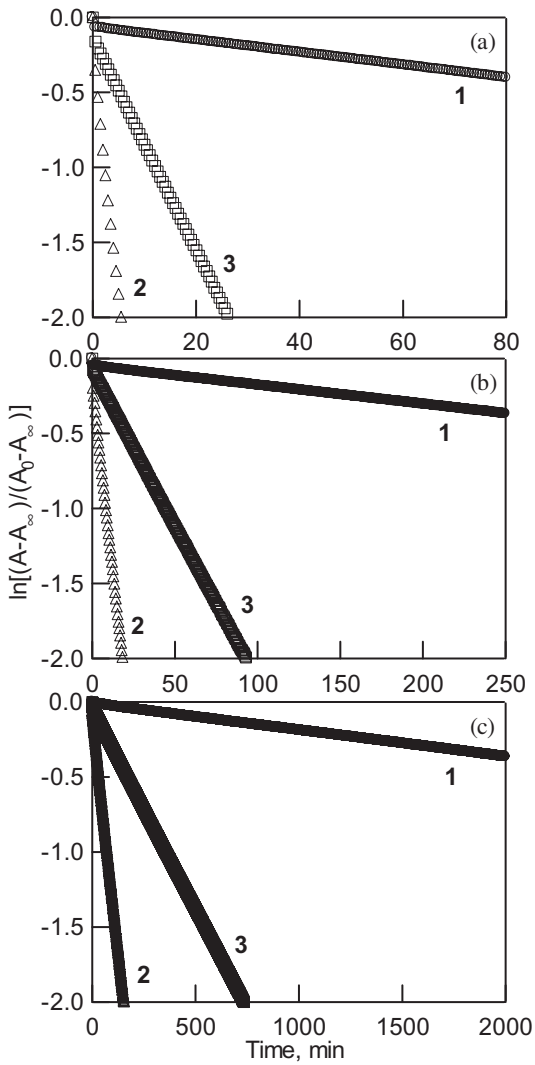

Fig. 4. Kinetic plots for demetalation of Zn 3,7-diformyl-chlorin **1** (open circle), Zn 3-formyl-chlorin **2** (open triangle), and Zn 7-formyl-chlorin **3** (open square) in acetone/water (3/1, vol/vol) at the proton concentration of 1.8×10^{-1} (a), 1.2×10^{-1} (b), and 6.0×10^{-2} M (c). Absorbance changes were monitored at 472, 450, and 459 nm for **1–3**, respectively. A_0, A, and A_∞ are Soret absorbance of Zn chlorins at the onset of measurements, at time t, and at the complete demetalation, respectively

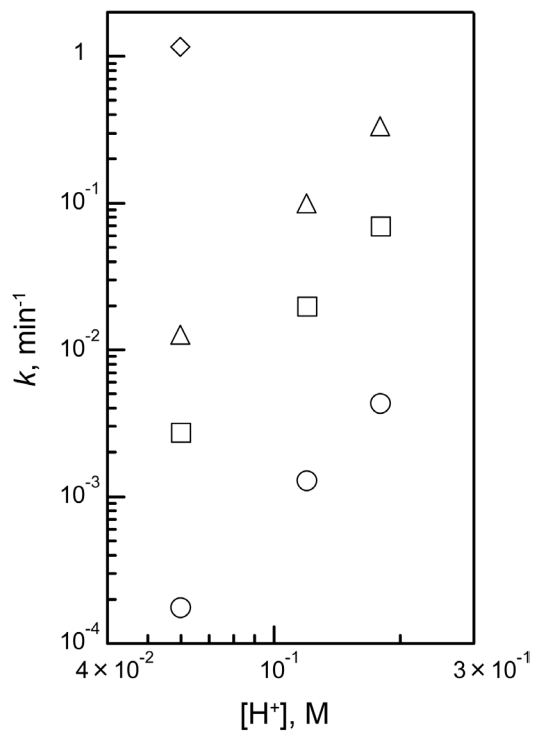

Fig. 5. Demetalation rate constants of Zn 3,7-diformyl-chlorin **1** (open circle), Zn 3-formyl-chlorin **2** (open triangle), Zn 7-formyl-chlorin **3** (open square), and Zn chlorin **4** (open diamond) in acetone/water (3/1, vol/vol) dependent on the examined proton concentrations

proton concentrations, which were *ca*. 10^{-1} M and *ca*. 10^{-2} M, respectively.

Effects of formyl groups in the A- and B-rings

Comparison of demetalation kinetics among Zn chlorins **1–4** revealed that formylated Zn chlorins **1–3** exhibited slower demetalation kinetics than **4** possessing no formyl group. These results can be ascribed to the electron-withdrawing ability of a formyl group, resulting in decrease of electron densities on core nitrogen atoms of the chlorin macrocycle [32, 35, 39]. Among the three Zn formylated chlorins **1–3**, the demetalation kinetics of Zn 3,7-diformyl-chlorin **1** was the slowest at the proton concentrations between 1.8×10^{-1} and 6.0×10^{-2} M, as seen in Figs 4 and 5. The relative ratios of demetalation rate constants of **1** to those of **2** and **3** were 0.013–0.014 and 0.062–0.065, respectively. These indicate that two formyl groups directly linked to the chlorin macrocycle result in significantly slower demetalation kinetics than one formyl group. Therefore, the effects of an electron-withdrawing formyl group on demetalation of chlorophyllous pigments can be amplified by increase of the number of formyl groups on the chlorin macrocycle. Such a combination effect of two formyl substituents linked to the different rings of the chlorin macrocycle on demetalation kinetics of chlorophyllous pigments was first demonstrated, although the effects of sole formyl group have been reported [22–24, 27, 28, 30–32, 34, 35, 39]. The relative ratio of demetalation rate constants of 3-formylated **2** over 7-formylated **3** were estimated to be 4.6–5.0 under the acidic conditions. We reported that this difference was ascribable to the aliphatic groups in the A- and B-rings, namely the 7-methyl group in **2** and 3-vinyl group in **3** [35]. Actually, dehydrogenation of the ethyl group to the vinyl group makes demetalation kinetics of metallochlorins slow down [35, 39].

To make the effects of formyl groups conjugated to the chlorin macrocycle on demetalation properties more clear, relationships between demetalation rate constants of Zn chlorins **1–4** and the sum of Hammett σ parameters [41] of the 3- and 7-substituents were investigated. Figures 6 and 7 show dependence of log *k* on the sum of Hammett σ_m and σ_p parameters, respectively. High correlations can be observed between log *k* of these Zn chlorins and Hammett σ_m constants: correlation coefficients $|r| = 0.999$, 0.998, and 0.990 at the proton concentrations of 1.8×10^{-1}, 1.2×10^{-1}, and 6.0×10^{-2} M, respectively (Fig. 6). Hammett σ_p constants were also correlated with log *k*: $|r| = 0.989$, 0.987, and 0.989 at the proton concentration of 1.8×10^{-1}, 1.2×10^{-1}, and 6.0×10^{-2} M, respectively (Fig. 7). Such high correlations reveal that demetalation properties of chlorophyllous pigments can be quantitatively explained by invoking combination of inductive effects of substituents in the A- and B-rings of the chlorin macrocycles. We reported the high correlations of the demetalation rate constants

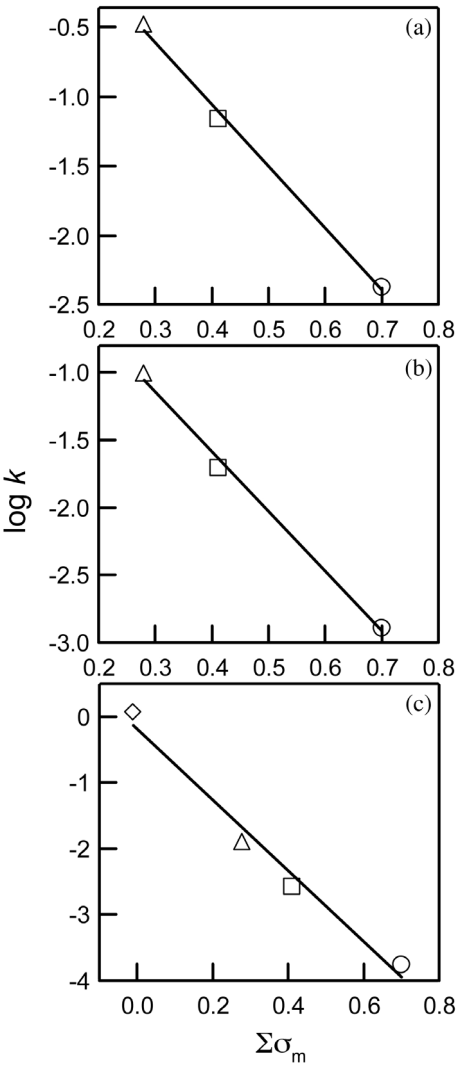

Fig. 6. Dependence of demetalation rate constants of Zn 3,7-diformyl-chlorin **1** (open circle), Zn 3-formyl-chlorin **2** (open triangle), Zn 7-formyl-chlorin **3** (open square), and Zn chlorin **4** (open diamond) at the proton concentrations of 1.8×10^{-1} (a), 1.2×10^{-1} (b), and 6.0×10^{-2} M (c) on the sum of Hammett σ_m constants of the 3- and 7-substituents

and Hammett σ parameters of the 3-substituents in Zn chlorins [39]. This study suggests that the quantitative effects of electron-withdrawing and -donating strength of the substituents linked to the chlorin macrocycle upon demetalation properties can apply to not only sole group but also multiple substituents of chlorophyllous pigments.

The slopes in Figs. 6 and 7 indicate susceptibility of reactions to electronic effects, namely Hammett ρ constants. Demetalation reactions of the Zn chlorins exhibited that ρ values were -4.4, -4.4, and -5.4 at the proton concentrations of 1.8×10^{-1}, 1.2×10^{-1}, and 6.0×10^{-2} M, respectively, against σ_m parameters (Fig. 6). Hammett ρ constants were estimated to be -3.0, -3.0, and -3.7 at the proton concentrations of 1.8×10^{-1},

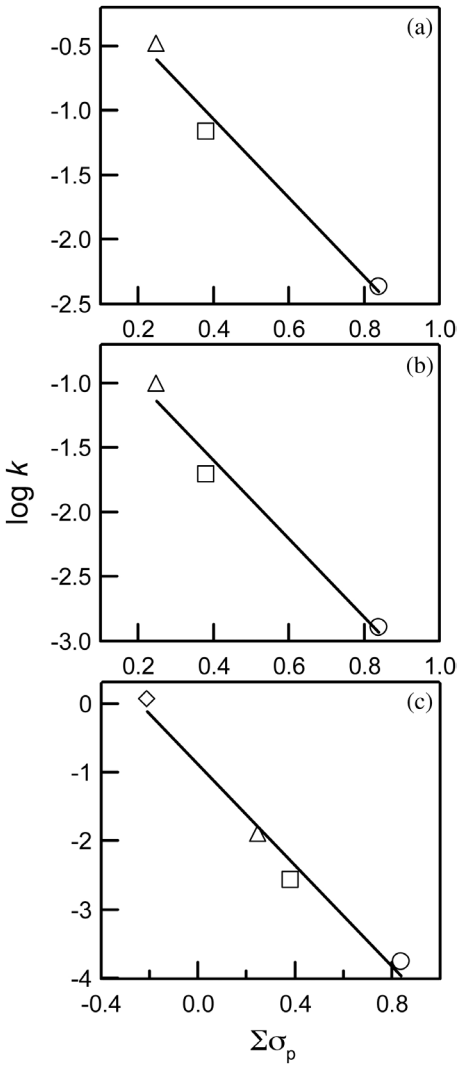

Fig. 7. Dependence of demetalation rate constants of Zn 3,7-diformyl-chlorin **1** (open circle), Zn 3-formyl-chlorin **2** (open triangle), Zn 7-formyl-chlorin **3** (open square), and Zn chlorin **4** (open diamond) at the proton concentrations of 1.8×10^{-1} (a), 1.2×10^{-1} (b), and 6.0×10^{-2} M (c) on the sum of Hammett σ_p constants of the 3- and 7-substituents

1.2×10^{-1}, and 6.0×10^{-2} M, respectively, against σ_p parameters (Fig. 7). The negative ρ values indicate the electrophilic attack of protons to core nitrogen atoms at the rate-determining steps in these reactions. The ρ values estimated in this study were somewhat different from those estimated in previous reports [34, 39], in which Hammett ρ values of the 3-substituted and 7-substituted Zn chlorins were distributed between -6.1 and -6.7 against σ_m, and between -4.1 and -4.9 against σ_p. One possible reason for the difference would be ascribable to the difference in proton concentrations of demetalation reactions. Further studies will be required to understand effects of reaction conditions and molecular structures on Hammett ρ constants in demetalation reactions of chlorophyllous pigments.

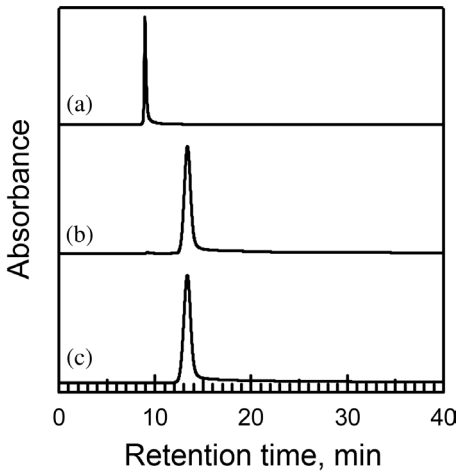

Fig. 8. HPLC elution patterns of Zn 3,7-diformyl-chlorin **1** before demetalation reaction (a), its reaction products after demetalation reaction in acetone/water (3/1, vol/vol) at the proton concentration of 1.8×10^{-1} M for 23 h (b), and synthesized free-base 3,7-diformyl chlorin **1′** (c). Pigments were eluted on a reverse-phase column $3C_{18}$-EB (4.6 mmϕ × 150 mm) with methanol at a flow rate of 0.3 mL.min^{-1} at 40 °C. Chromatograms (a), (b), and (c) were recorded at 469, 450, and 450 nm, respectively

HPLC analysis

The products after demetalation reactions under the conditions in Fig. 3 were analyzed by reverse-phase HPLC. Figure 8 depicts HPLC elution patterns of Zn 3,7-diformyl-chlorin **1** before incubation in acidic aqueous acetone and its reaction products after the incubation. A fraction at 9 min before incubation was assigned to Zn 3,7-diformyl-chlorin **1** (Fig. 8a). After incubation for 23 h, a main product, which had the Soret and Q_y-bands at 450 and 677 nm, respectively, in the HPLC eluent, was detected at 13 min (Fig. 8b). This fraction was ascribed to free-base 3,7-diformyl-chlorin **1′**, since synthesized **1′**, which was thoroughly characterized by ^{1}H NMR, HRMS, and visible absorption spectroscopy, was eluted at the same retention time (Fig. 8c). A slight fraction, which would be a by-product during the demetalation reaction, was detected at 9 min in this chromatogram (Fig. 8b). HPLC analyses of the products after demetalation reactions of the other two monoformylated chlorins **2** and **3** have sole fraction under the acidic conditions (data not shown). The HPLC analysis revealed that few side-reactions occurred within the reaction time in which demetalation rate constants were estimated under the present reaction conditions.

EXPERIMENTAL

Apparatus

Visible absorption spectra were measured with a Shimadzu UV-2450 spectrophotometer, where the

reaction temperature was regulated with a Shimadzu thermo-electric temperature-controlled cell holder TCC-240A. High-performance liquid chromatography (HPLC) was performed with a Shimadzu LC-20AT pump, an SPD-M20A or SPD-20AV detector, and a CTO-20A column oven. Mass spectra (MS) were measured with a JEOL JMS700 spectrometer; *m*-nitorobenzyl alcohol was used as a matrix. High-resolution mass spectra (HRMS) were measured with a JEOL GC-mate II spectrometer; *m*-nitorobenzyl alcohol and glycerol were used as matrixes. ^{1}H NMR spectra were measured with a JEOL JNM-AL400 NMR spectrometer; chemical shifts were expressed (in ppm) relative to chloroform (7.26 ppm) as an internal reference.

Synthesis

Synthesis of diformylated Zn chlorin 1. To a THF solution (20 mL) of methyl pyropheophorbide *b* (**3**, 16.7 mg), which was prepared from Chl *b* [34, 39], two pieces of microcapsulated OsO_4 [42], which was purchased from Wako Chemical Industries, Ltd., was added at 0 °C. A solution of $NaIO_4$ (0.25 g) and CH_3COOH (0.32 mL) in H_2O (2.0 mL) was dropped into the ice-chilled THF solution, and stirred overnight at room temperature. After extraction of reaction products with CH_2Cl_2 several times, the combined organic phases were washed with $NaHCO_3$-saturated water and distilled water, dried over anhydrous Na_2SO_4, and evaporated under reduced pressure. The residue was purified by flash silica gel column chromatography and recrystallized from CH_2Cl_2 and hexane to give methyl 3-devinyl-3-formyl-pyropheophorbide *b.* **3,7-diformyl-chlorin 1′.** 8.7 mg, 52% yield. ^{1}H NMR ($CDCl_3$): δ, ppm 11.44, 10.95 (each 1H, s, 3-, 7-CHO), 10.38, 9.36, 8.76 (each 1H, s, 5-, 10-, 20-H), 5.33, 5.17 (each 1H, d, J = 20 Hz, 13^2-H_2), 4.57 (1H, dq, J = 2, 7 Hz, 18-H), 4.39 (1H, dt, J = 9, 3 Hz, 17-H), 3.86–3.74 (2H, m, 8-CH_2), 3.69, 3.67, 3.63 (each 3H, s, 2-, 12-, 17^4-CH_3), 2.84–2.75, 2.70–2.62, 2.45–2.27 (1H + 1H + 2H, m, 17-CH_2CH_2), 1.94 (3H, d, J = 7 Hz, 18-CH_3), 1.66 (3H, t, J = 8 Hz, 8^1-CH_3), -0.60, -2.49 (each 1H, s, NH). UV-vis (acetone): λ_{max}, nm 675 (relative intensity, 0.20), 617 (0.04), 535 (0.08), 449 (1.00), 431 (0.48). HRMS (FAB): *m/z* found 564.2363, calcd. for $C_{33}H_{32}N_4O_5$ $[M]^+$, 564.2373. Free-base chlorin **1′** (17.7 mg) was dissolved in CH_2Cl_2 (9 mL) and $Zn(CH_3COO)\cdot 2H_2O$-saturated methanol (4 mL) was added to the CH_2Cl_2 solution, followed by stirring for 8 h. The solution was neutralized by aq. 4% $NaHCO_3$, washed with distilled water several times, dried over anhydrous Na_2SO_4, and evaporated under reduced pressure. The residue was recrystallized from CH_2Cl_2 and hexane to afford Zn methyl 3-devinyl-3-formyl-pyropheophorbide *b.* **Zn 3,7-diformyl-chlorin 1.** 14.8 mg, 75% yield. ^{1}H NMR ($CDCl_3$): δ, ppm 11.05, 10.70 (each 1H, s, 3-, 7-CHO), 10.04, 9.49, 8.53 (each 1H, s, 5-, 10-, 20-H), 5.01, 4.88 (each 1H, d, J = 20 Hz, 13^2-H_2), 4.51–4.45 (1H, m, 18-H), 4.33–4.28 (1H, m, 17-H), 3.96–3.86 (2H, m, 8-CH_2), 3.58, 3.51, 3.32 (each 3H, s, 2-, 12-, 17^4-CH_3), 2.65–2.58, 2.56–2.44, 2.30–2.22 (1H + 2H + 1H, m, 17-CH_2CH_2), 1.91 (3H, d, J = 6 Hz, 18-CH_3), 1.67 (3H, t, J = 7 Hz, 8^1-CH_3). UV-vis (acetone): λ_{max}, nm 659 (relative intensity, 0.26), 606 (0.05), 558 (0.04), 463 (1.00), 437 (0.27). HRMS (FAB): *m/z* found 626.1555, calcd. for $C_{33}H_{30}N_4O_5Zn$ $[M]^+$, 626.1508.

Synthesis of Zn chlorins 2–4. Zn methyl pyropheophorbide *d* (Zn 3-formyl-chlorin **2**) and Zn methyl pyropheophorbide *a* (Zn chlorin **4**) were prepared from Chl *a* according to previous reports [34, 39, 43, 44]. Zn methyl pyropheophorbide *b* (Zn 7-formyl-chlorin **3**) was prepared from Chl *b* [34]. **Zn 3-formyl-chlorin 2.** UV-vis (acetone): λ_{max}, nm 680 (relative intensity, 0.95), 630 (0.12), 586 (0.08), 541 (0.04), 443 (1.00), 390 (0.48). MS (FAB): *m/z* found 612.4, calcd. for $C_{33}H_{32}N_4O_4Zn$ $[M]^+$, 612.2. **Zn 7-formyl-chlorin 3.** UV-vis (acetone): λ_{max}, nm 637 (relative intensity, 0.30), 587 (0.07), 451 (1.00). MS (FAB): *m/z* found 624.4, calcd. for $C_{34}H_{32}N_4O_4Zn$ $[M]^+$, 624.2. **Zn chlorin 4.** UV-vis (acetone): λ_{max}, nm 655 (relative intensity, 0.69), 607 (0.11), 568 (0.06), 524 (0.04), 425 (1.00), 405 (0.60), 379 (0.37). MS (FAB): *m/z* found 610.3, calcd. for $C_{34}H_{34}N_4O_3Zn$ $[M]^+$, 610.2.

Measurements of demetalation kinetics

A 3.0 mL acetone solution of Zn chlorins **1–4** (Soret absorbance = 1.0 at the 1-cm pathlength) was mixed with a 1.0 mL distilled water containing hydrochloric acid. The proton concentration was calculated by assuming complete dissociation of hydrochloric acid in a mixture of acetone and water (3/1, vol/vol), since previous reports ensured such dissociation at the proton concentration up to *ca*. 10^{-1} M [27, 29]. Demetalation kinetics was examined by monitoring the absorbances at the Soret peak positions of Zn chlorins at the proton concentration of 1.8×10^{-1}, 1.2×10^{-1}, and 6.0×10^{-2} M for **1–3**, as well as 6.0×10^{-2} M for **4** under the control of reaction temperature at 25 °C.

Pigment analyses after demetalation reaction

After demetalation reactions, the solution was neutralized by $NaHCO_3$-saturated water. The reaction products were extracted with CH_2Cl_2, washed with NaCl-saturated water, and dried over anhydrous Na_2SO_4. The solution was filtrated and dried with nitrogen gas. The residue was analyzed by reverse-phase HPLC column $3C_{18}$-EB (4.6 mmϕ × 150 mm, Nacalai Tesque, Inc., Kyoto, Japan) with methanol at a flow rate of 0.3 $mL.min^{-1}$ at 40 °C.

CONCLUSION

This study reveals effects of the formyl groups conjugated to the A- and B-rings of the chlorin macrocycle

on kinetics stabilities against removal of the central metal from the chlorin ring by using diformylated and monoformylated Zn chlorins. Zn chlorins possessing two formyl groups in both the A- and B-rings exhibited significantly slow demetalation kinetics by combination effects of both the formyl groups. The effects of the two formyl groups in the chlorin macrocycle on demetalation kinetics can be quantitatively rationalized by combination of their electron-withdrawing ability, judged from high correlations between the demetalation rate constants and the sum of Hammett σ parameters of the 3- and 7-substitutients on the chlorin macrocycle. The present results will help to understand demetalation reactions of natural Chl pigments and synthetic cyclic tetrapyrrole molecules.

Acknowledgements

We thank Prof. Tomohiro Miyatake and Mr. Yohei Masuda, Ryukoku University, for HRMS measurements, and Ms. Keiko Kinoshita, Kinki University, for experimental assistance. This work was partially supported by a Grant-in-Aid for Scientific Research (C) (No. 23550201) (to YS) from the Japan Society for the Promotion of Science. KS was supported by a JSPS Fellowship for Young Scientists.

REFERENCES

1. Scheer H. In *Chlorophylls and Bacteriochlorophylls: Biochemistry, Biophysics, Functions and Applications*, Grimm B, Porra RJ, Rüdiger W and Scheer H. (Eds.) Springer: Dordrecht, 2006; pp. 1–26.
2. Tamiaki H and Kunieda M. In *Handbook of Porphyrin Science*, Vol. 11, Kadish KM, Smith KM and Guilard R. (Eds.) World Scientific: Singapore, 2011; pp. 223–290.
3. Miyashita H, Ikemoto H, Kurano N, Adachi K, Chihara M and Miyachi S. *Nature* 1996; **383**: 402.
4. Murakami A, Miyashita H, Iseki M, Adachi K and Mimuro M. *Science* 2004; **303**: 1633.
5. Chen M, Schliep M, Willows RD, Cai Z-L, Neilan BA and Scheer H. *Science* 2010; **329**: 1318.
6. Groe A, Pfennig N, Brockmann Jr. H and Trowizsch W. *Arch. Microbiol.* 1975; **102**: 103.
7. Vogl K, Tank M, Orf GS, Blankenship RE and Bryant DA. *Front. Microbiol*. 2012; **3**: DOI:10.3389/fmicb.2012.00298.
8. Harada J, Mizoguchi T, Tsukatani Y, Noguchi M and Tamiaki H. *Sci. Rep.* 2012; **2**: 671. DOI:10.1038/srep00671.
9. Tsuchiya T, Mizoguchi T, Akimoto S, Tomo T, Tamiaki H and Mimuro M. *Plant Cell Physiol.* 2012; **53**: 518.
10. Tsuchiya T, Akimoto S, Mizoguchi T, Watabe K, Kindo H, Tomo T, Tamiaki H and Mimuro M. *Biochim. Biophys. Acta* 2012; **1817**: 1285.
11. Saga Y and Tamiaki H. *Chem. Biodivers.* 2012; **9**: 1659.
12. Klimov VV, Klevanik AV, Shuvalov VA and Krasnovsky AA. *FEBS Lett.* 1977; **82**: 183.
13. Klimov VV, Shuvalov VA and Heber U. *Biochim. Biophys. Acta* 1985; **809**: 345.
14. Hastings G, Durrant JR, Barber J, Porter G and Klug DR. *Biochemistry* 1992; **31**: 7638.
15. Loll B, Kern J, Saenger W, Zouni A and Biesiadka J. *Nature* 2005; **438**: 1040.
16. Feher G, Allen JP, Okamura MY and Rees DC. *Nature* 1989; **339**: 111.
17. Deisenhofer J, Epp O, Miki K, Huber R and Michel H. *Nature* 1985; **318**: 618.
18. Kräutler B and Matile P. *Acc. Chem. Res.* 1999; **32**: 35.
19. Hörtensteiner S. *Annu. Rev. Plant Biol.* 2006; **57**: 55.
20. Kräutler B. *Photochem. Photobiol. Sci.* 2008; **7**: 1114.
21. Hörtensteiner S and Kräutler B. *Biochim. Biophys. Acta* 2011; **1807**: 977.
22. Mackinney G and Joslyn MA. *J. Am. Chem. Soc.* 1940; **62**: 231.
23. Mackinney G and Joslyn MA. *J. Am. Chem. Soc.* 1941; **63**: 2530.
24. Schanderl SH, Chichester CO and Marsh GL. *J. Org. Chem.* 1962; **27**: 3865.
25. Rosoff M and Aron C. *J. Phys. Chem.* 1965; **69**: 21.
26. Berezin BD, Drobysheva AN and Karmanova LP. *Russ. J. Phys. Chem.* 1976; **50**: 720.
27. Mazaki H and Watanabe T. *Bull. Chem. Soc. Jpn.* 1988; **61**: 2969.
28. Mazaki H, Watanabe T, Takahashi T, Struck A and Scheer H. *Bull. Chem. Soc. Jpn.* 1992; **65**: 3212.
29. Kobayashi M, Yamamura M, Akiyama M, Kise H, Inoue K, Hara M, Wakao N, Yahara K and Watanabe T. *Anal. Sci.* 1998; **14**: 1149.
30. Saga Y, Hirai Y and Tamiaki H. *FEBS Lett.* 2007; **581**: 1847.
31. Hirai Y, Tamiaki H, Kashimura S and Saga Y. *Photochem. Photobiol.* 2009; **85**: 1140.
32. Hirai Y, Tamiaki H, Kashimura S and Saga Y. *Photochem. Photobiol. Sci.* 2009; **8**: 1701.
33. Saga Y, Hojo S and Hirai Y. *Bioorg. Med. Chem.* 2010; **10**: 5697.
34. Hirai Y, Kashimura S and Saga Y. *Photochem. Photobiol.* 2011; **87**: 302.
35. Hirai Y, Sasaki S, Tamiaki H, Kashimura S and Saga Y. *J. Phys. Chem. B* 2011; **115**: 3240.
36. Saga Y, Miura R, Sadaoka K and Hirai Y. *J. Phys. Chem. B* 2011; **115**: 11757.
37. Gerola AP, Tsubone TM, Santana A, de Oliveira HPM, Hioka N and Caetano W. *J. Phys. Chem. B* 2011; **115**: 7364.
38. Saga Y, Hirai Y, Sadaoka K, Isaji M and Tamiaki H. *Photochem. Photobiol.* 2013; **89**: 68.

39. Saga Y, Kobashiri Y and Sadaoka K. *Inorg. Chem.* 2013; **52**: 204.
40. Miyashita H, Adachi K, Kurano N, Ikemoto H, Chihara M and Miyachi S. *Plant Cell Physiol*. 1997; **38**: 274.
41. Hansch C, Leo A and Taft RW. *Chem. Rev*. 1991; **91**: 165.
42. Nagayama S, Endo M and Kobayashi S. *J. Org. Chem*. 1998; **63**: 6094.
43. Tamiaki H, Amakawa M, Shimono Y, Tanikaga R, Holzwarth AR and Schaffner K. *Photochem. Photobiol.* 1996; **63**: 92.
44. Saga Y and Otono T. *Chem. Lett.* 2012; **41**: 360.